Algerian Journal of Research and Technology
https://doi.org/10.58681/ajrt.21050201
A.J.R.T Volume 5 (N°2) (2021) 1 - 14

Numerical Simulation of NO_x Removal in $N_2/O_2/H_2O/CO_2$ Mixture Under Different Reduced Electric Fields

K. Ferouani [1,2,*], M. Lemerini [1], M. Bouzar [1]

[1]*LPT, Université A. Belkaid, Faculté des Sciences, 13000, Tlemcen, Algérie.*

[2]*Ecole Supérieure des Sciences Appliquées. BP 165 RP Bel Horizon 13000 Tlemcen, Algérie.*

* *Corresponding author. ferouani_karim@yahoo.fr*

Received. March 21, 2020. Accepted. March 03, 2021. Published. December 22, 2021.

DOI: https://doi.org/10.58681/ajrt.21050201

Abstract. Nitric oxides (NO and NO_2) and SO_2 emissions are major environmental problems because of their negative influence on human health and vegetation. The federal regulations on limiting the pollution emitted by the engines of motor vehicles have triggered intense research on new techniques for the removal of these pollutants.
In this work, analyze the time behavior of different species and their reaction rates using a model based on chemical kinetics equations. The considered model can describe the behavior of twenty different chemical species participating in one hundred selected chemical reactions. A large number of investigations considered the removal of NO_x showing the effects of N, O, and O_3 radicals, and also an analysis of other species such as negative ions O^-_2, O^-_3, O^-_4, and radicals O_3, OH presents in $N_2/O_2/H_2O/CO_2$ mixture. In particular, we analyze the time evolution of the rate coefficient and depopulation rate of certain reactions. We have found that the rate of depopulation of NO and NO_2 is substantially affected by the reduced electric field rise from 100–200 Td.

Keywords. Chemical kinetic, Rate reaction, NO_x removal, Reduced electric field.

INTRODUCTION

Nowadays, gas discharge plasmas and their applications in chemistry, electrochemistry, biology, and environmental programs are being widely studied. They can be used for reforming treasonous pollutants, such as NO_x, CO_x, and SO_x. These studies are based on the simulation of reactors for the reduction of NOx gases (Hatakeyama et al., 2001; Yoshida et al., 2009; Balogh et al., 2001; Even et al., 1993; Jawork et al., 2009).

The removal of NO_x (including NO and NO_2) and SO_2 has become a central scientific concern because of its key role in many global environmental problems such as acid rain. In addition, NO and SO_2 contribute to the degradation of visibility since they form accumulation mode aerosol particles containing nitrates and sulfates. There are also adverse effects on human health. In higher concentrations, these chemical species may cause bronchitis or pneumonia (Prather and Logan, 1994).

While the emission of SO_2 can be limited by using low-Sulphur fuels, NO_x is an ozone precursor and one of the most difficult air pollutants to suppress, which remains a serious hazard to human health. A major source of NO_x emissions is the exhaust gases of motor vehicles, especially from diesel engines (Lepperhoff et al., 1994).

Therefore, restrictive federal regulations on limiting pollution have triggered intense research on new techniques for NO_x removal. To meet these new limits, one option is the treatment of exhaust gases with corona discharges in plasma reactors (Ferouani et al., 2010; Ferouani et al., 2015).

Several previous studies have already shown the effect of non-equilibrium discharges at atmospheric pressure gas dynamics (Spyrou et al., 1992; Eichwald et al., 1997). These effects can be dynamic (collective movement of drift) and /or thermal (uncoordinated movements). The charged particles and in particular the ions drift their movement exchange between the electrodes of the quantity of the neutral fluid movement and gives it a drift motion.

The fluid motion induced by an electric discharge is usually called electric wind or ion wind it was demonstrated long ago (Chang, 2008), and has been widely studied in the case of a corona discharge between a pointe-plane (Loiseau, 2002; Zhao and Adamiak, 2005). As a result, of the discharge, the charged particles (positive ions, negative ions, or electrons) are created in the inter-electrode space. These species are accelerated by the electric field by Coulomb force and drawn towards the cathode to the positive ions and the anode, for the electrons and negative ions.

In all cases, the momentum of the gas can modify the development of the discharge to the extent that all the critical phenomena depend on the reduced field E/N where N is the density of neutral gas (Flitti and Pancheshnyi, 2009). These processes increase the internal energy of the neutral gas. During the discharge phase, the gas temperature around the pointe can quickly reach 800−1000 °K (Katsuki et al., 2006).

During the phase of post-discharge, the vibrational energy reservoir gradually relaxes causing slight warming of the ionized channel and a local reduction in the gas density.

In this work, we simulate the time behavior of different species and their reaction rates model based on chemical kinetics equations.

Analysis concerns twenty chemical species (molecules N_2, O_2, H_2O, CO_2, OH, HO_2, HNO_3, O_3), atoms N, O, H, nitric oxides NO, NO_2, NO_3, N_2O_5, and negative ions (O^-_2, O^-_3, O^-_4, NO^-_2, NO^-_3), in the mixture (N_2: 76, O: 18%, H_2O: 3% and CO_2: 3%). These different species react following 100 selected chemical reactions and the analysis concerns six values of the reduced electric field (100,120,140,160,180,200 Td).

In this numerical simulation, we suppose various effects induced by the passage of a corona discharge in a mixed gas. For the sake of simplification, we assume that the gas has no convective movement gradients and the pressure remains constant.

MATHEMATICAL MODEL

The mathematical model used consists of a system of equations that takes into account the variation of the density and the chemical kinetics of the environment. To model the no thermal plasma, we have designed a numerical code of zero-order to solve the transport equations of particle charges and neutral particles. This algorithm is based on the integration of a system of equations under consideration.

The conservation equations of the density of each species:

The equation for the density of species in the mixture can be written:

$\frac{\partial n_i}{\partial t} = S_j(T)$(1)

n: the density of species *I*, $\frac{\partial n_i}{\partial t}$*:* the time rate of change of density, $S_j(T)$: sources term.

n: the total density of the gas is given by the classical equation of a perfect gas:

$P = n\mathrm{k_B}T$ (2)

Where *P* represents the pressure in Pascal, $\mathrm{k_B}$ Boltzmann constant, and *T* the absolute temperature (in Kelvin).

Modelling of chemical kinetics:

The reactivity of the gas is taken into account in the source term of each equation $S_j(T)$ conservation density (1).

In the case where chemical reactions where two bodies $S_j(T)$ are given a time by the relation:

$S_j(T) = \sum_\alpha \pm K_\alpha(T)(n_q n_p)_\alpha$ (3)

$K_\alpha(T)$: the coefficient of the chemical reaction number, $(n_q n_p)$: the product of densities of species *p* and *q* interacting in response to the reaction, positive and negative signs that are similar to the reactions of formation or disappearance of specie *j*. If we have three bodies so the term source is given by the product of the density of the former.

The coefficients of reactions are made under the form of Arrhénus (Eichwald et al., 1997):

$K_\alpha(T) = \mathrm{K}T^{\eta}\exp(-\theta/T)$ (4)

K, η, θ, are three coefficients of adjustment (θ is the activation energy of the T is the absolute temperature of the species involved in the warm rain that has left the chemical reaction α).

RESULTS AND DISCUSSION

The chemical kinetics involves 20 different chemical species: molecules N_2, O_2, H_2O, CO_2, OH, HO_2, HNO_3, O_3, atoms N, O, H, nitric oxides NO, NO_2, NO_3, N_2O_5, and negative ions (O^-_2, O^-_3 O^-_4, NO^-_2, NO^-_3), in the mixture (N_2: 76% O_2 18%, H_2O: 3% and CO_2: 3%). These different species react following 100 selected chemical reactions the main ones are given in table 1.

Table 1. The main plasma reactions generate the main radical to remove NO_x and their rate constants. (Rate constants are in units of $cm^3 \cdot molecule^{-1} \cdot s^{-1}$ for two-body actions ad $cm^6 molecule^{-2} \cdot s^{-1}$ for three-body reactions. T is the gas temperature in Kelvin).

Reactions		Rate constants	References
R1	$NO + NO_3 \rightarrow NO_2 + NO_2$	$k1 = 2 \times 10^{-11}$	(Kossyi et al., 1992)
R2	$NO + O_3 \rightarrow O_2 + NO_2$	$k2 = 1.8 \times 10^{-12}$	(Kossyi et al., 1992)
R3	$NO + O^-_3 \rightarrow NO^-_2 + O_2$	$k3 = 2.0 \times 10^{-12}$	(Kossyi et al., 1992)
R4	$NO + O^-_3 \rightarrow NO^-_3 + O$	$k4 = 1.0 \times 10^{-10}$	(Kossyi et al., 1992)
R5	$NO + O^-_4 \rightarrow NO^-_3 + O_2$	$k5 = 2.5 \times 10^{-10}$	(Kossyi et al., 1992)
R6	$NO + HO_2 \rightarrow NO_2 + OH$	$k6 = 13.5 \times 10^{-11}$	(Kossyi et al., 1992)
R7	$NO_2 + O^-_2 \rightarrow NO^-_2 + O_2$	$k7 = 7.0 \times 10^{-10}$	(Eichwald et al., 2002)
R8	$NO_2 + OH \rightarrow HNO_3$	$k8 = 13.5 \times 10^{-11}$	(Eichwald et al., 2002)
R9	$NO_2 + O^-_3 \rightarrow NO^-_2 + O_3$	$k9 = 7 \times 10^{-10}$	(Eichwald et al., 2002)
R10	$NO_2 + N \rightarrow NO + NO$	$k10 = 2.3 \times 10^{-12}$	(Eichwald et al., 2002)
R11	$NO_3 + OH \rightarrow HO_2 + NO_2$	$k11 = 2.35 \times 10^{-11}$	(Eichwald et al., 2002)
R12	$NO_3 + HO_2 \rightarrow HNO_3 + O_2$	$k12 = 4.05 \times 10^{-12}$	(Eichwald et al., 2002)
R13	$NO_3 + NO_3 \rightarrow O_2 + NO_2 + NO_2$	$k13 = 1.2 \times 10^{-15}$	(Sieck et al., 2000)
R14	$NO_3 + O \rightarrow O_2 + NO_2$	$k\ 14 = 1.7 \times 10^{-11}$	(Sieck et al., 2000)
R15	$N + O_2 \rightarrow O + NO$	$k15 = 8.9 \times 10^{-17}$	(Kossyi et al., 1992)
R16	$N + NO_2 \rightarrow N_2 + O_2$	$k16 = 7 \times 10^{-13}$	(Kossyi et al., 1992)
R17	$N + NO^-_3 \rightarrow NO + NO_2 + e$	$k17 = 5.0 \times 10^{-10}$	(Kossyi et al., 1992)
R18	$NO_2 + NO_3 + O_2 \rightarrow N_2O_5 + O_2$	$k18 = 3.7 \times 10^{-30}$	(Kossyi et al., 1992)
R19	$O_3 + H \rightarrow OH + O_2$	$k19 = 2.8 \times 10^{-11}$	(Mok et al., 1998)
R20	$OH + H_2 \rightarrow H_2O + H$	$k20 = 6.7 \times 10^{-15}$	(Mok et al., 1998)
R21	$OH + O_3 \rightarrow HO_2 + O_2$	$k21 = 6.5 \times 10^{-14}$	(Mok et al., 1998)
R22	$OH + HO_2 \rightarrow H_2O + O_2$	$k22 = 1.1 \times 10^{-10}$	(Mok et al., 1998)
R23	$OH + HNO_3 \rightarrow NO_3 + H_2O$	$k23 = 1.3 \times 10^{-13}$	(Mok et al., 1998)
R24	$H_2O + e \rightarrow OH + H + e$	$k24 = 2.6 \times 10^{-12}$	(Mok et al., 1998)
R25	$CO_2 + e \rightarrow CO + O + e$	$k25 = 8.7 \times 10^{-10}$	(Mok et al., 1998)

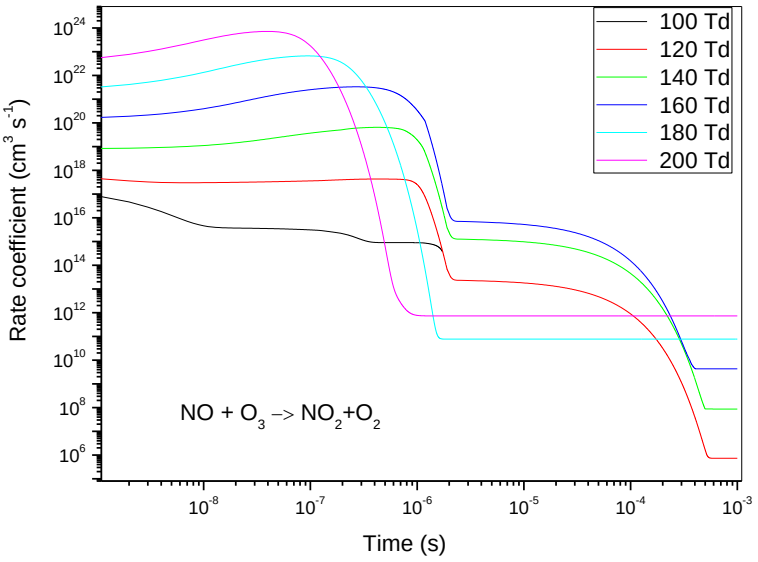

Fig.1. Time evolution of rate coefficient of reaction R2.

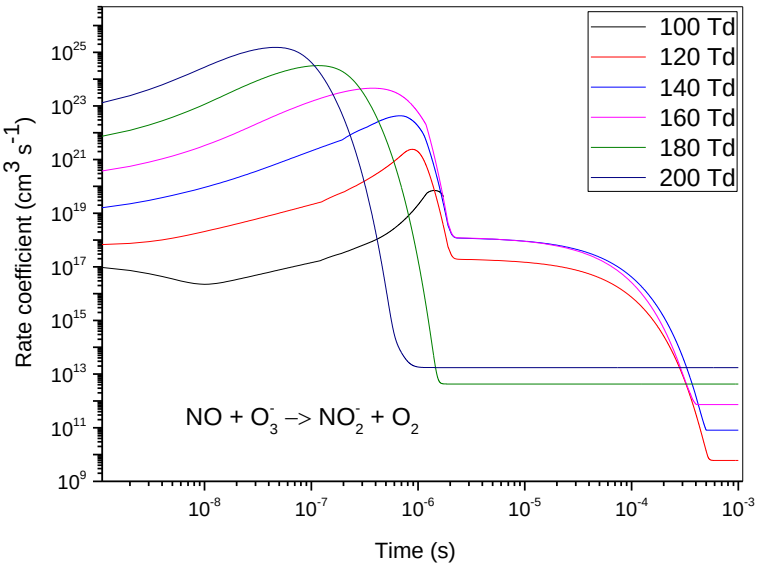

Fig.2. Time evolution of rate coefficient of reaction R3.

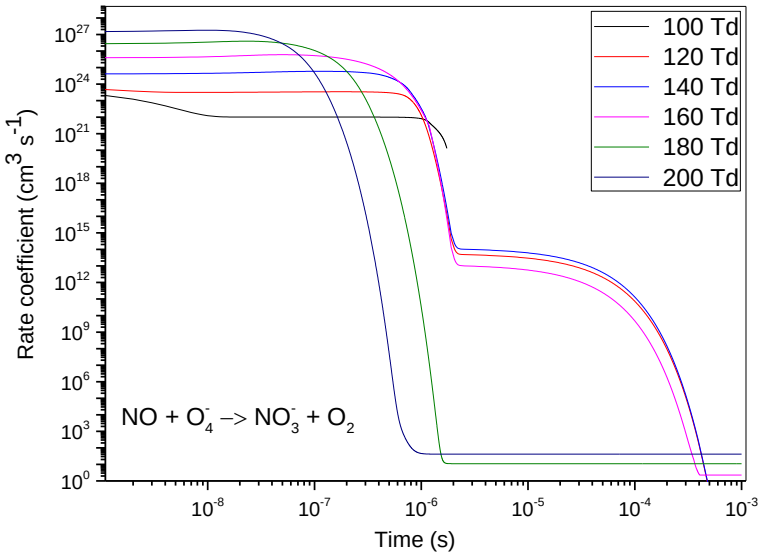

Fig. 3. Time evolution of rate coefficient of reaction R5.

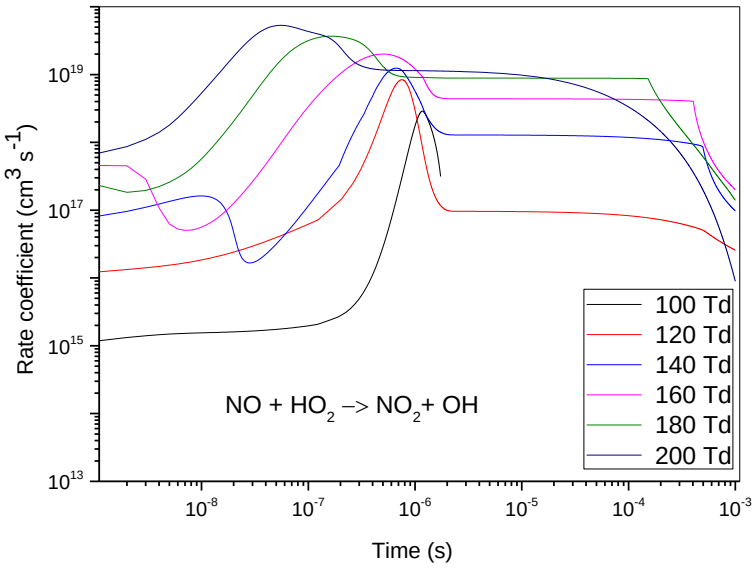

Fig. 4. Time evolution of rate coefficient of reaction R6.

Figure 5 shows the time evolution of depopulation rate $(n_0\text{-}n)/n_0$, where n_0 represents the initial density and n the density values between 10^{-9} –10^{-3}s of NO species in mixture $N_2/O_2/H_2O/CO_2$ for different reduced electric fields (100 –200 Td). We presented in this figure the results of the competition between all participants' reactions to oxide nitrogen reduction.

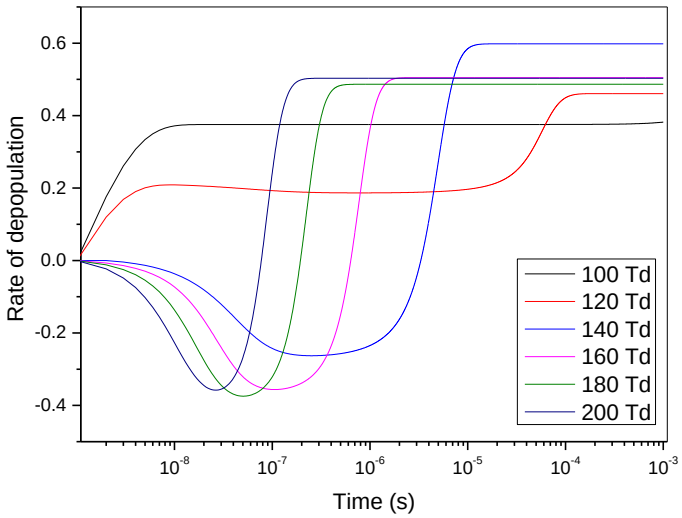

Fig. 5. Time evolution of depopulation rate of NO species in mixture $N_2/O_2/H_2O/CO_2$.

We observe the influence of the reduced electric field on NO reduction. It is noted for low values of the reduced electric field 100 Td and 120 Td an average reduction of 10% caused by the overall reaction, while for high value 180 Td we observed that the rate of reduction reached 70%. Finally, NO reduction (R2, R3, R5, and R6) largely depends on the radical concentration of O_3, O^-_3, O^-_4, and HO_2. In the beginning, the NO consumption is not significant because the O^-_3, O^-_4, and HO_2 radicals generated react mostly with NO_x and their concentration remains low. In the following section, we will analyze the effects of oxidizing radicals O^-_2, O^-_3, N, and OH on removing NO_2 and NO_3 species, which represent the oxide nitrogen to the main NO_x. We calculate in particular the rate coefficient of reactions R7, R8, R9, and R10 between 10^{-9} –10^{-3} s. According to Table 1, these reactions are the main reactions to removing the NO_2 species. We notice that these species react with O^-_2, O^-_3, N, OH to form especially O_2, O_3, NO^-_2, NO, and HNO_3. As for the oxide nitrogen results, we notice that the reaction rate shown in figures 6 until 9, is related to the increase of the reduced electric field. In addition, we notice to all of these curves that the reactions become less effective after $t=4x10^{-4}$ s except for the reaction R9 where the influence goes up to 10^{-3} s.

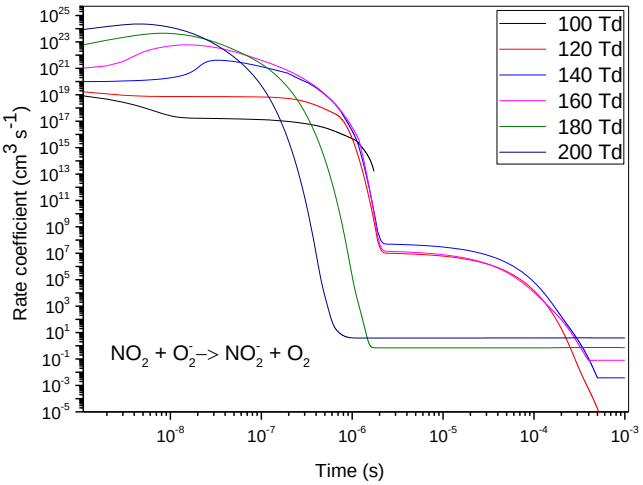

Fig. 6. Time evolution of rate coefficient o action R7.

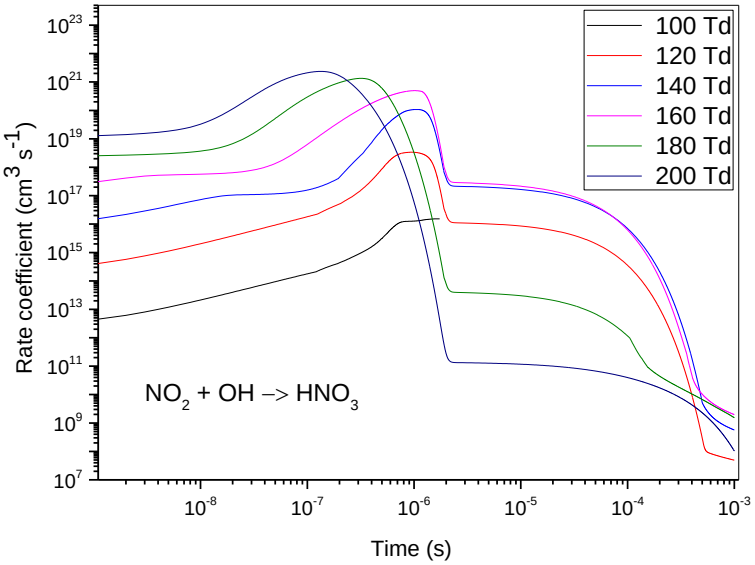

Fig. 7. Time evolution of rate coefficient of reaction R8.

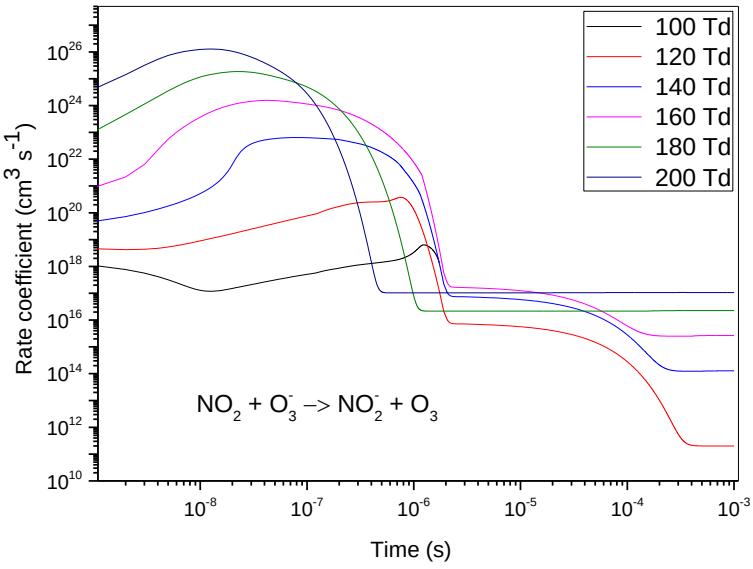

Fig. 8. Time evolution of rate coefficient of reaction R9.

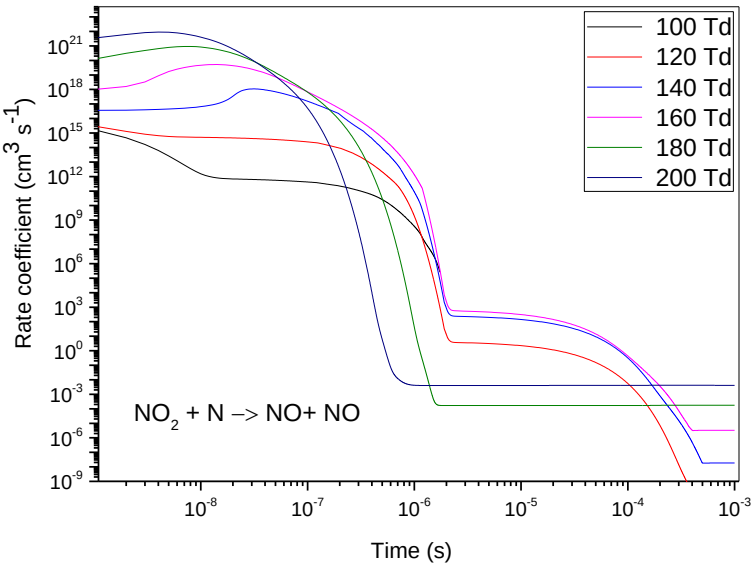

Fig. 9. Time evolution of rate coefficient of reaction R10.

Figure 10 shows the time evolution of the population rate of NO_2 for various values of reduced electric fields (100 - 200 Td). Unlike the previous, result for oxide nitrogen, we obese for NO_2 a different behavior. Firstly, we notice in the beginning from 10^{-9} –10^{-8} s, a significant reduction (80% an average) especially for 100 –120 Td which stabilizes at this value until the end. Secondly, at 140 –180 Td, there is a different behavior, for example when the reduced electric field equals 140Td the depopulation rate decreases and reaches approximately 20% at $5x10^{-8}$s. Then, there was an increase that reached 70% on average at the moment $5x10^{-8}$ s followed by a reduction (25%) until the end.

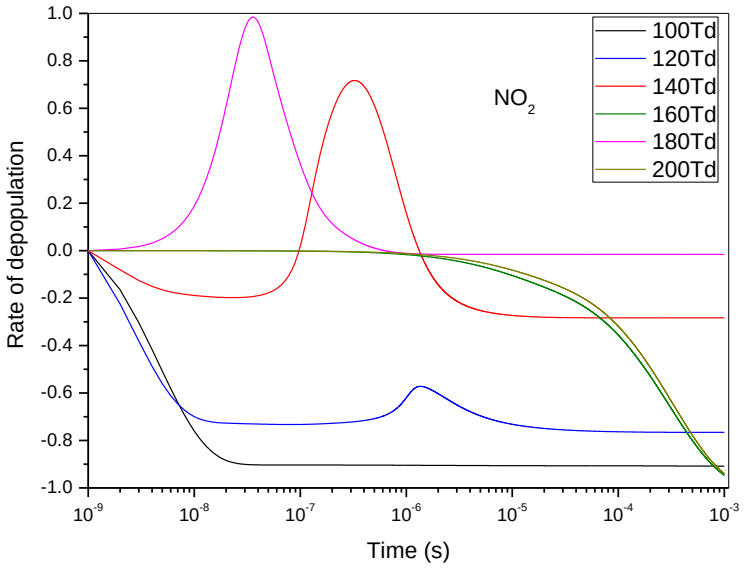

Fig. 10. Time evolution of depopulation rate of species dies in mixture $N_2/O_2/H_2O/CO_2$.

In figures 11 to 14, we will complete this analysis with radicals O, OH, and HO_2 on removing NO_3 species. According to Table 1, we notice that R11 to R14 react with these radicals to form especially O_2, O_3, HO_2, and NO_2. We observe on these curves the strong and significant influence of these reactions until time $t = 2x10^{-6}$ s. After this moment, the influence of these reactions diminishes or stabilizes until the end.

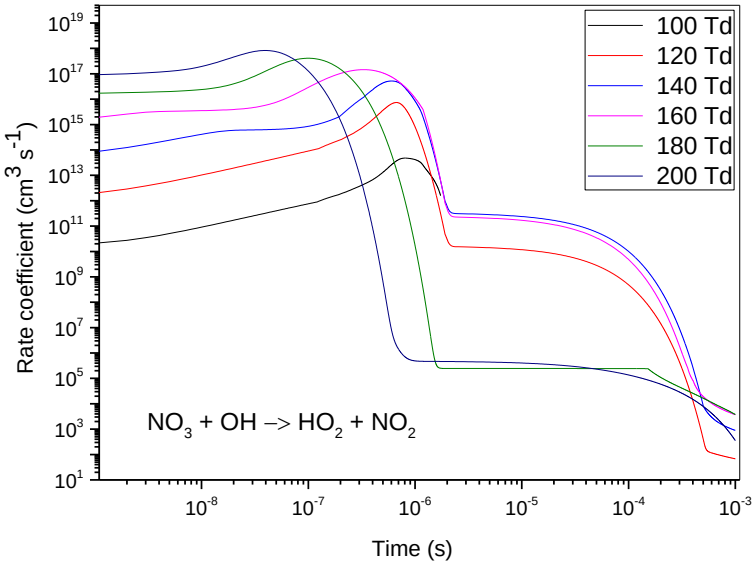

Fig. 11. Time evolution of rate coefficient of reaction R11.

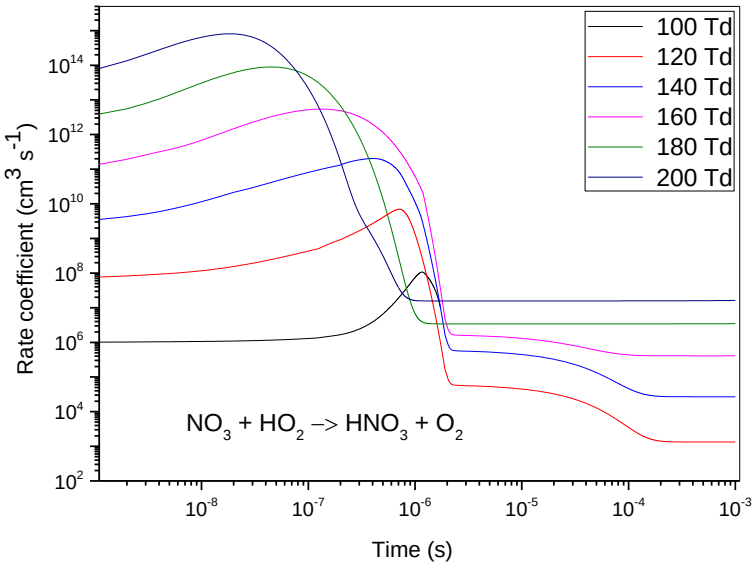

Fig. 12. Time evolution of rate coefficient of reaction R12.

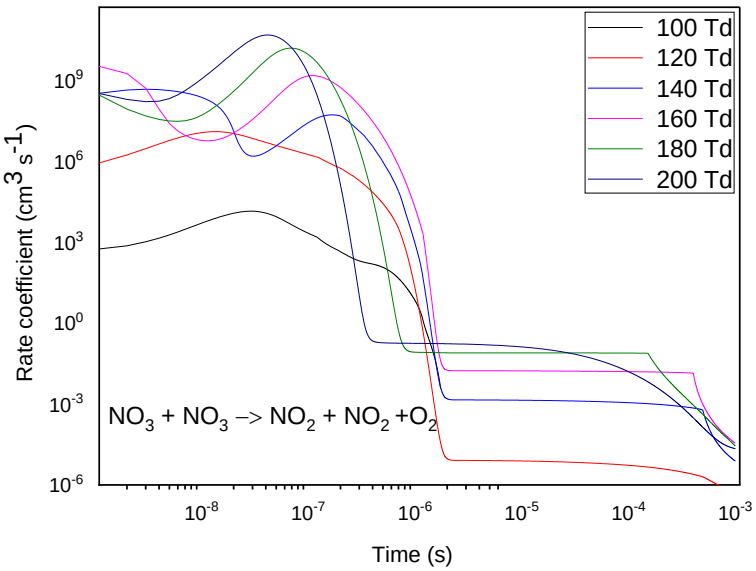

Fig. 13. Time evolution of rate coefficient of reaction R13.

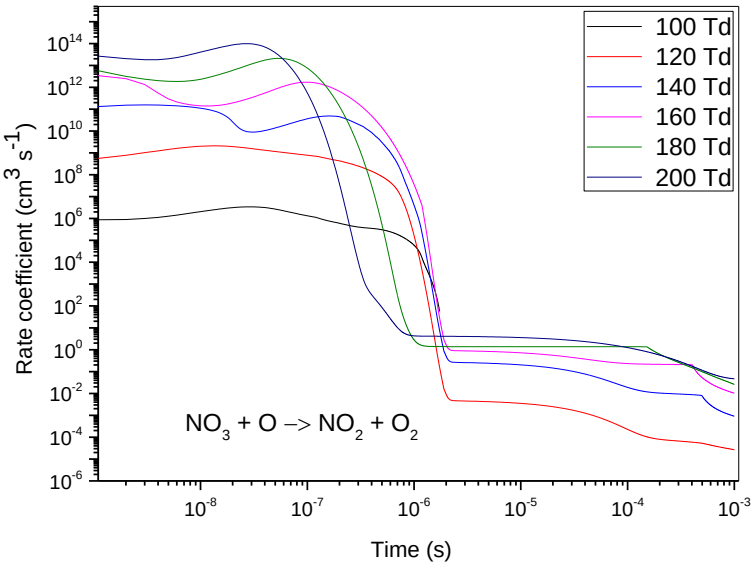

Fig. 14. Time evolution of rate coefficient of reaction R14.

Figure 15 shows the depopulation rate of the NO_3 species under the same conditions as above. It is noted a creation followed by consumption for 100, 120, and 140 Td. The rate of production reached 90% on average for these three values until 10^{-7} s, then decreases down to zero till the end of time. We observe unusually for 160 and 200 Td a balance between production and reduction of this species up to 10^{-5} s, then the rate decreases. Unlike other values, when the reduced electric field equals 180 Td, the density of NO_3 decreases until $2x10^{-8}$s and the depopulation rate reaches approximately 75%, then the density increases until $2x10^{-7}$ s where the rate variation exceeds 80%, then the density drops again and the rate reaches 90% and stabilizes at this value.

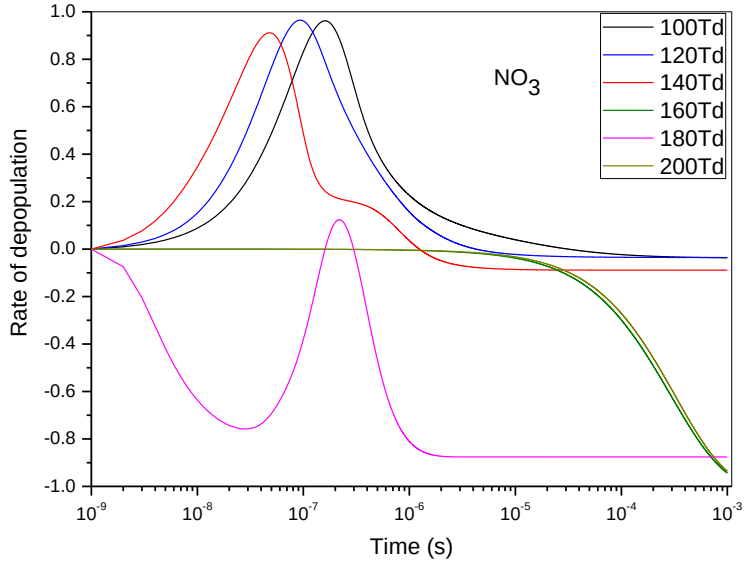

Fig. 15. Time evolution of depopulation rate of NO_3 species in mixture $N_2/O_2/H_2O/CO_2$.

CONCLUSIONS

In this work, a zero-dimensional model based on equations of kinetics was successfully applied to study the temporal variations of certain reactions, which participate in NOx removal involved in $N_2/O_2/H_2O/CO_2$ mixed gas under different reduced electric fields. The results show two types of evolution, which depends strongly on the increase of reduced electric field:

(1) The reduction of oxides of nitrogen is different for all species. It is observed that the increase and decrease of these species are different and dep strongly on the values of reduced electric fields.

(2) We also notice the creation of other species that participate more or less in this chemical kinetics such as HNO_3.

Finally, the fractions of the energy transferred from charged to neutral particles via elastic and inelastic processes are given from a Boltzmann equation solution. Therefore, the fraction of energy lost during elastic, excitation, and ionization processes in the same gas mixture depends on the electric reduced field. For example, at low values less than 120 Td, the energy loss is due to rotational and vibration collisions, whereas for values more than 120 Td the energy loss is mainly due to electronic excitation and ionization collisions.

REFERENCES

Balogh, R. M., Ionel, I., Stepan, D., Rabl, H. P., & Pfaffinger, A. (2011). NOx reduction using Selective Catalytic Reduction (SCR) system–α variation test. *Termotehnica*, *2*, 38-42.

Chang, J. S. (2008). Physics and chemistry of plasma pollution control technology. *Plasma Sources Science and Technology*, *17*(4). https://doi.org/10.1088/0963-0252/17/4/045004

Eichwald, O., Guntoro, N. A., Yousfi, M., & Benhenni, M. (2002). Chemical kinetics with electrical and gas dynamics modelization for NOx removal in an air corona discharge. *Journal of Physics D: Applied Physics*, *35*(5). https://doi.org/10.1088/0022-3727/35/5/305

Eichwald, O., Yousfi, M., Hennad, A., & Benabdessadok, M. D. (1997). Coupling of chemical kinetics, gas dynamics, and charged particle kinetics models for the analysis of NO reduction from flue gases. *Journal of Applied Physics*, *82*(10). https://doi.org/10.1063/1.366336

Evans, D., Rosocha, L. A., Anderson, G. K., Coogan, J. J., & Kushner, M. J. (1993). Plasma remediation of trichloroethylene in silent discharge plasmas. *Journal of Applied Physics*, *74*(9). https://doi.org/10.1063/1.354241

Ferouani, A. K., Lemerini, M., & Belhour, S. (2010). Numerical modelling of nitrogen thermal effects produced by the negative dc corona discharge. *Plasma Science and Technology*, *12*(2). https://doi.org/10.1088/1009-0630/12/2/15

Ferouani, A. K., Lemerini, M., Merad, L., & Houalef, M. (2015). Numerical Modelling Point-to-Plane of Negative Corona Discharge in N2 Under Non-Uniform Electric Field. *Plasma Science and Technology*, *17*(6). https://doi.org/10.1088/1009-0630/17/6/06

Flitti, A., & Pancheshnyi, S. (2009). Gas heating in fast pulsed discharges in N2-O2 mixtures. *EPJ Applied Physics*, *45*(2). https://doi.org/10.1051/epjap/2009011

HATAKEYAMA, K., TANABE, S., HAYASHI, Y., MATSUMOTO, H., & FUTAMI, H. (2001). NOx decomposition by discharge plasma reactor. *Journal of Advanced Science*, *13*(3). https://doi.org/10.2978/jsas.13.459

Jaworek, A., Krupa, A., Lackowski, M., Sobczyk, A. T., Czech, T., Ramakrishna, S., Sundarrajan, S., & Pliszka, D. (2009). Nanocomposite fabric formation by electrospinning

and electrospraying technologies. *Journal of Electrostatics*, *67*(2–3). https://doi.org/10.1016/j.elstat.2008.12.019

Katsuki, S., Tanaka, K., Fudamoto, T., Namihira, T., Akiyama, H., & Bluhm, H. (2006). Shock waves due to pulsed streamer discharges in water. *Japanese Journal of Applied Physics, Part 1: Regular Papers and Short Notes and Review Papers*, *45*(1 A). https://doi.org/10.1143/JJAP.45.239

Kossyi, I. A., Kostinsky, A. Y., Matveyev, A. A., & Silakov, V. P. (1992). Kinetic scheme of the non-equilibrium discharge in nitrogen-oxygen mixtures. *Plasma Sources Science and Technology*, *1*(3). https://doi.org/10.1088/0963-0252/1/3/011

Loiseau, J. F., Batina, J., Noël, F., & Peyrous, R. (2002). Hydrodynamical simulation of the electric wind generated by successive streamers in a point-to-plane reactor. *Journal of Physics D: Applied Physics*, *35*(10). https://doi.org/10.1088/0022-3727/35/10/310

Mok, Y. S., Ham, S. W., & Nam, I. S. (1998). Mathematical analysis of positive pulsed corona discharge process employed for removal of nitrogen oxides. *IEEE Transactions on Plasma Science*, *26*(5). https://doi.org/10.1109/27.736063

Prather, M. J., & Logan, J. A. (1994). Combustion's impact on the global atmosphere. *Symposium (International) on Combustion*, *25*(1). https://doi.org/10.1016/S0082-0784(06)80796-4

Sieck, L. W., Heron, J. T., & Green, D. S. (2000). Chemical kinetics database and predictive schemes for humid air plasma chemistry. Part I: Positive ion - molecule reactions. *Plasma Chemistry and Plasma Processing*, *20*(2). https://doi.org/10.1023/A:1007021207704

Spyrou, N., Held, B., Peyrous, R., Manassis, C., & Pignolet, P. (1992). Gas temperature in a secondary streamer discharge: An approach to the electric wind. *Journal of Physics D: Applied Physics*, *25*(2). https://doi.org/10.1088/0022-3727/25/2/013

Yoshida, K., Rajanikanth, B. S., & Okubo, M. (2009). NOx Reduction and Desorption Studies Under Electric Discharge Plasma Using a Simulated Gas Mixture: A Case Study on the Effect of Corona Electrodes. *Plasma Science and Technology*, *11*(3). https://doi.org/10.1088/1009-0630/11/3/15

Zhao, L., & Adamiak, K. (2005). EHD flow in air produced by electric corona discharge in pin-plate configuration. *Journal of Electrostatics*, *63*(3-4 SPEC. ISS.). https://doi.org/10.1016/j.elstat.2004.06.003